

# Coalescence Behavior of Gold Nanoparticles

Y. Q. Wang · W. S. Liang · C. Y. Geng

Received: 17 November 2008 / Accepted: 9 March 2009 / Published online: 20 March 2009  
© to the authors 2009

**Abstract** The tetraoctylammonium bromide (TOAB)-stabilized gold nanoparticles have been successfully fabricated. After an annealing of the as-synthesized nanoparticles at 300 °C for 30 min, the coalescence behavior of gold nanoparticles has been investigated using high-resolution transmission electron microscopy in detail. Two types of coalescence, one being an ordered combination of two or more particles in appropriate orientations through twinning, and the other being an ordered combination of two small particles with facets through a common lattice plane, have been observed.

**Keywords** Gold nanoparticles · Coalescence · Faceting

## Introduction

Low-dimensional quantum structures have shown to have unique optical and electronic properties. In particular, the shape and size of low-dimensional structures are crucial parameters that determine those physical properties [1, 2]. The characterization of these parameters is an important issue either in fundamental research or in technological applications, covering from fabrication and characterization to device processing. Among nanostructures, metallic nanoparticles such as gold and silver particles are also

important because some of their main physical properties might be completely different from the corresponding ones in either molecules or bulk solids. Therefore, it is essential to investigate the size and shape of metallic nanoparticles, especially for gold nanoparticles.

In our earlier paper [3], we reported the fabrication and microstructure of Au–Cu<sub>2</sub>O nanocube heterostructures. Transmission electron microscopy (TEM) observations show that there are also intact gold nanoparticles apart from these nanocube heterostructures. The coarsening of gold nanoparticles during the annealing is usually attributed to Ostwald ripening [4], in which the crystal growth takes place by diffusion of atoms between neighboring nanoparticles. Recent studies [5–7] of TiO<sub>2</sub> and ZnS nanocrystals growing under hydrothermal conditions have shown that the oriented attachment or coalescence plays an important role in the coarsening of nanocrystals. In addition, the coalescence of small particles by twinning was also reported in FePt and Si nanocrystals [8–10]. In the process of the oriented attachment or coalescence, the nanoparticles can themselves act as the building blocks for crystal growth. For gold nanoparticles, no detailed investigation on the coalescence behavior has been carried out using high-resolution transmission electron microscopy (HRTEM).

## Experimental

Gold nanoparticles were synthesized via a modification of a literature protocol [11, 12]. Briefly, an aqueous solution of HAuCl<sub>4</sub> · 3H<sub>2</sub>O (0.03 M, 6 mL) was added to a solution of TOAB in toluene (0.15 M, 6 mL). The yellow aqueous phase became colorless, and the toluene phase turned orange as a result of phase transfer and complexing of

---

Y. Q. Wang (✉) · W. S. Liang · C. Y. Geng  
The Cultivation Base for State Key Laboratory, Qingdao University, No. 308 Ningxia Road, Qingdao 266071, People's Republic of China  
e-mail: yqwang@qdu.edu.cn

$[\text{AuCl}_4]^-$  with tetraoctylammonium cations. After stirring for 10 min at room temperature, a freshly prepared aqueous solution of sodium borohydride,  $\text{NaBH}_4$  (0.26 M, 6 mL) was added dropwise into the reaction mixture over a period of 30 min, after which the mixture was vigorously stirred for additional 30 min. Subsequently, the organic phase was separated and was washed with 1%  $\text{H}_2\text{SO}_4$  once and then with distilled-deionised water five times. Finally, the organic phase was dried using  $\text{MgSO}_4$  and filtered through a filter paper. The as-synthesized gold nanoparticles were characterized using conventional TEM and HRTEM. The specimen for TEM observation was prepared by evaporating a drop (5  $\mu\text{L}$ ) of the nanoparticle dispersion onto a carbon-film-coated copper grid.

In order to investigate coalescence behavior of the gold nanoparticles, a copper grid covered with gold nanoparticles was placed in an oven and the temperature was raised to and kept constant at 300 °C for 30 min. After the annealing, the gold nanoparticles were extensively examined using HRTEM. The bright-field (BF) imaging, selected-area electron diffraction (SAED) and HRTEM were carried out using a field emission gun (FEG) transmission electron microscope operating at 200 kV.

## Results and Discussion

Figure 1a shows a typical BF image of the as-synthesized gold nanoparticles. It can be seen that most nanoparticles (>90%) are spherical. The right-upper inset is the corresponding SAED pattern, which confirms that the particles are of pure gold. TEM analysis of the diameters of 250 nanoparticles yields an average diameter of 5.2 nm. The polydispersity of these nanoparticles is 1.1 nm. After the annealing at 300 °C for 30 min, the morphologies of gold nanoparticles changed drastically. Figure 1b shows a typical high-angle annular dark-field (HAADF) image of the nanostructures formed after the annealing [3]. From Fig. 1b, we can see that there are two types of nanostructures, one being nanoparticles, and the other being the nanocubes. The right-lower inset is the corresponding SAED pattern obtained from this sample, which can be indexed using the lattice parameters of  $\text{Cu}_2\text{O}$  ( $a = 4.269 \text{ \AA}$ ) and gold ( $a = 4.09 \text{ \AA}$ ), confirming the existence of  $\text{Cu}_2\text{O}$  and gold. We have already reported the fabrication and microstructure of these nanocubes in [3], and will focus on the study of coalescence behavior of the gold nanoparticles here.

Extensive HRTEM observations demonstrate that most gold particles have an elongated shape and there are two types of coalescence. One type is that two or more small particles (without facets) coalesce into bigger ones through twinning, and the other type is that two particles (with

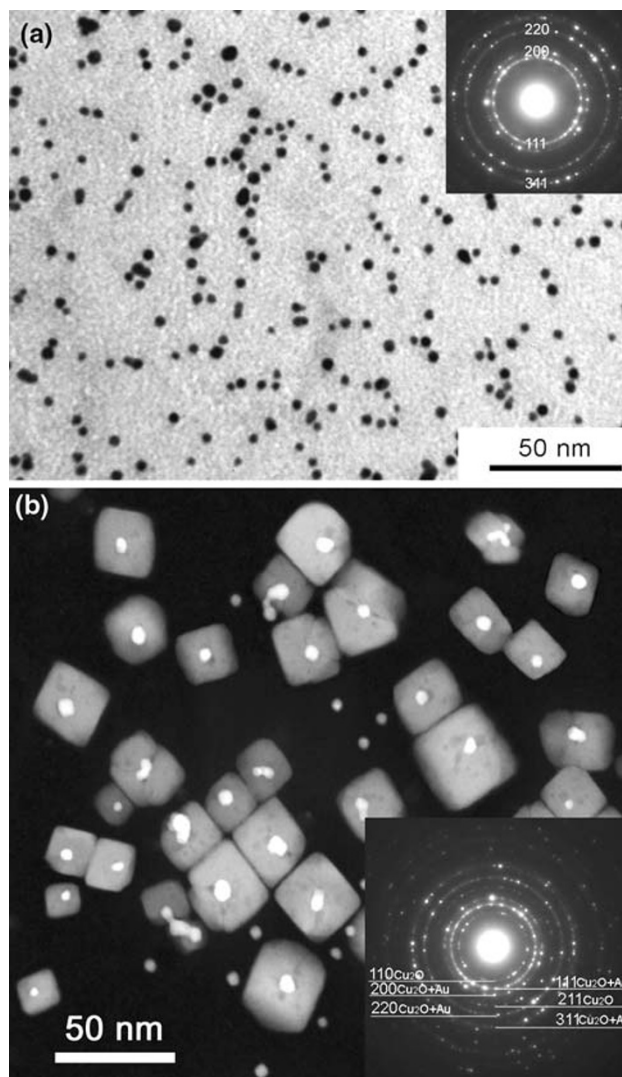
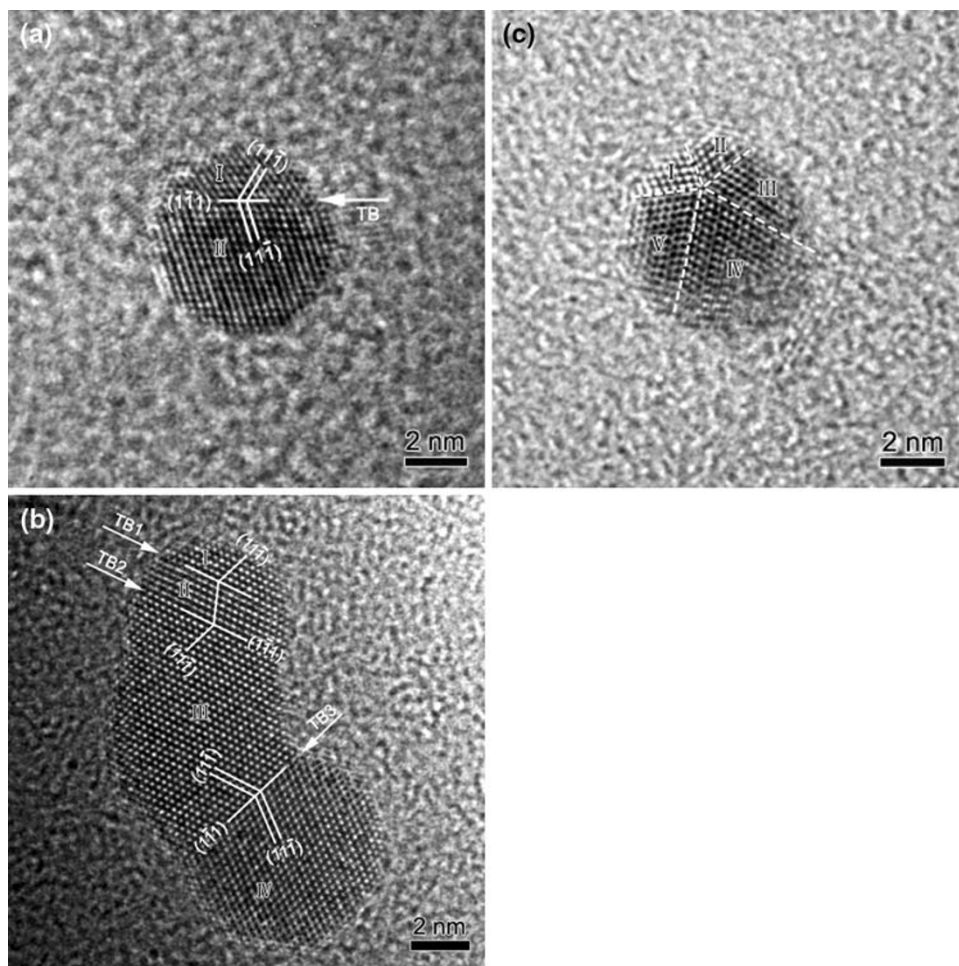


**Fig. 1** **a** Typical BF TEM image of gold nanoparticles before annealing, the *right-upper inset* is the corresponding SAED pattern. **b** Typical HAADF image of nanostructure after an annealing at 300 °C for 30 min [3], the *right-lower inset* is the corresponding SAED pattern

facets) combine together through a common lattice plane. The statistical analysis of more than 200 gold nanoparticles showed that the volume fraction of the nanoparticles with characteristics of the first-type coalescence is around 40%, while the volume fraction for those with characteristics of second-type coalescence is around 20%.

Figure 2 shows several examples of the first-type coalescence. Figure 2a shows an example of a gold particle (around 6 nm in diameter) with a single-twin structure, where the particle is oriented along [011]. The twinning elements are given in Fig. 2a, and the twin boundary is labeled with TB. From Fig. 2a, the lattice spacing for the {111} planes is measured to be 2.35 Å. This particle is slightly elongated, and nanograin I is smaller than

**Fig. 2** Coalescence of two or more gold particles (without facets) through  $\{111\}$  twinning. **a** A particle with a single-twin structure. **b** A particle with a triple-twin structure. **c** A particle with a fivefold twinning configuration



nanograin II. This particle can be regarded as a coalescence result of two small particles. Figure 2b shows a particle with a triple-twin structure, where the particle is viewed along  $[011]$ . The  $\{111\}$  lattice spacing is measured to be 2.36 Å. The particle is elongated, like a footprint. All the four nanograins are self-arranged by twinning in an ordered way. The triple twinning configuration has not been observed in gold nanoparticles before, and the formation of the observed twinning structure can be attributed to the coalescence of four small particles. From Fig. 2b, it can be seen that four small particles labeled with I, II, III, and IV connect each other through three twinning boundaries, and the twinning planes are  $\{111\}$ . The twin boundaries are indicated by white arrows labeled with TB1, 2 and 3. In addition, nanograins I and II consist of only six atomic planes. Figure 2c shows an example of a gold particle with a fivefold twinning structure, where the particle is oriented along  $[011]$ . For face-centered-cubic (fcc) gold, it is well known that the  $\{111\}$  twinning angle between two adjacent variants in equilibrium is  $70.53^\circ$  [13–15]. After fivefold twinning, there is still a mismatch angle of  $360^\circ - 70.53^\circ \times 5 = 7.35^\circ$  between the first and the fifth variant.

Due to the small size of these particles, the mismatch angle can be accommodated by lattice distortions, which can be clearly seen in Fig. 2c. The twinning boundaries are indicated by dashed lines in Fig. 2c. Each twin variant in the fivefold twin is marked with a number from I to V. This particle can also be regarded as the coalescence result of five small particles.

Figure 3 shows two examples of the second-type coalescence. Figure 3a shows an example of the coalescence of two nanoparticles with a projected shape of more or less a hexagon. The two particles have nearly the same size, around 6 nm. The two particles combine together with a common lattice plane of  $\{111\}$ . The  $\{111\}$  lattice spacing is measured to be 2.36 Å. The contour and facets of the coalesced particle are indicated by dashed lines in Fig. 3a. Figure 3b shows an example of the coalescence of two particles with a projected shape of a square. These two particles combine together through a common lattice plane of  $\{010\}$ . The two particles have nearly the same size, around 6 nm. The left particle is oriented close to a zone axis, while the right one is not. The contour and facets of the particle is shown in Fig. 3b. The lattice spacing

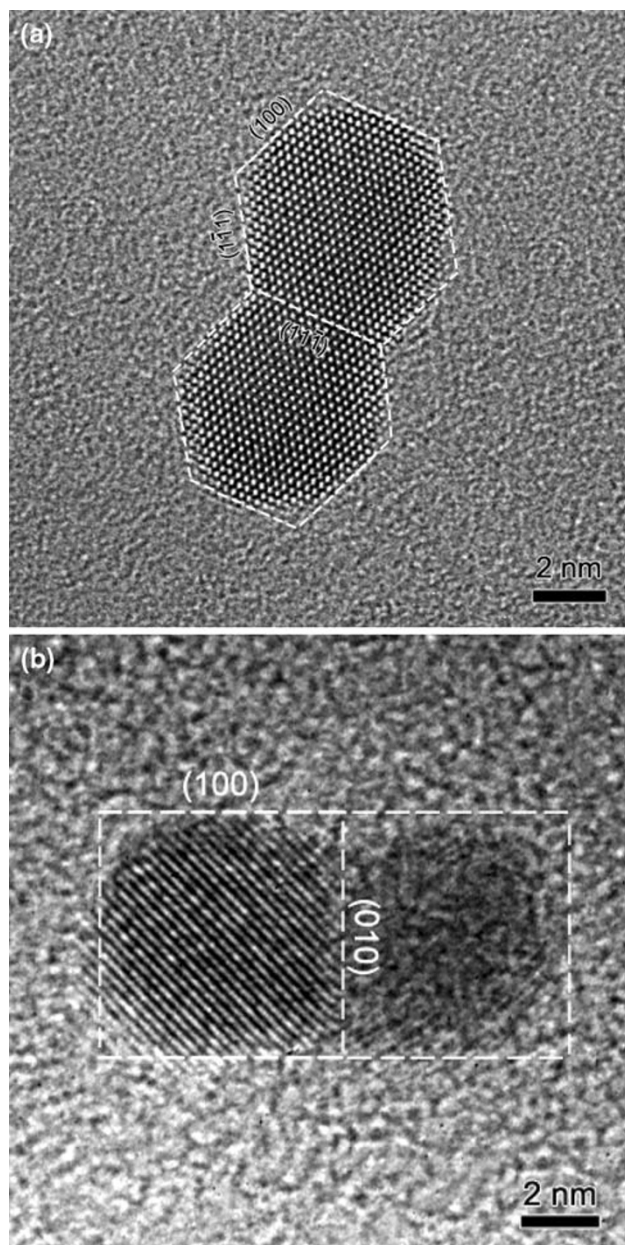


**Fig. 3** Coalescence of two particles with facets through a common lattice plane. **a** Coalescence of two particles with a projected shape of a hexagon. **b** Two particles with a projected shape of a square

measured from the left part of Fig. 3b is 2.89 Å, and the lattice fringes correspond to gold {110} planes. Here, we observed two lattice planes acting as the boundary, one being {111} and the other being {010}. These two planes have lower surface free energy than {110} planes in fcc gold. Compared with the coherent twinning boundary, these interfaces are more stable. Both particles in Fig. 3 show clear facets before coalescence. The precise role of facets on the nanoparticle surface in the coalescence process is a subject of interest. Both experiments [16] and

computer simulations [17] on two-dimensional islands suggest that the presence of facets can be effective in slowing down the coalescence process. Here, we observed that two particles join together through their common lattice planes, and the shape of the final particle is elongated along one dimension after coalescence.

As temperature increases, the TOAB stabilizing ligands melt and serve as solvent, and those gold nanoparticles which are situated close to each other can move around and start the coalescence process. As for the gold particles adopting which type of coalescence, it depends on the shapes of the initial particles, the concentration of particles put on the copper grid, their positions on the copper grid, and their crystal orientations.

## Conclusions

In summary, the coalescence behavior of gold nanoparticles has been investigated using HRTEM. Two types of coalescence, one being an ordered combination of two or more particles through twinning and the other being combination of two particles through a common lattice plane, have been observed.

**Acknowledgments** The authors would like to thank the financial support from Qingdao University. The project was supported by The Scientific Research Funding for the Introduced Talents (No. 06300701).

## References

- Z.L. Wang, *J. Phys. Chem. B* **104**, 1153 (2000)
- P. Buffat, J.P. Borel, *Phys. Rev. A* **13**, 2287 (1976). doi:10.1103/PhysRevA.13.2287
- Y.Q. Wang, K. Nikitin, D.W. McComb, *Chem. Phys. Lett.* **456**, 202 (2008). doi:10.1016/j.cplett.2008.03.027
- W. Ostwald, *Z. Phys. Chem. (Leipzig)* **34**, 495 (1900)
- R.L. Penn, J.F. Banfield, *Geochim. Cosmochim. Acta* **63**, 1549 (1999). doi:10.1016/S0016-7037(99)00037-X
- R.L. Penn, J.F. Banfield, *Science* **281**, 969 (1998). doi:10.1126/science.281.5379.969
- F. Huang, H.Z. Zhang, J.F. Banfield, *Nano Lett.* **3**, 373 (2003). doi:10.1021/nl025836+
- Z.R. Dai, S.H. Sun, Z.L. Wang, *Nano Lett.* **1**, 443 (2001). doi:10.1021/nl0100421
- Z.R. Dai, S.H. Sun, Z.L. Wang, *Surf. Sci.* **505**, 325 (2002). doi:10.1016/S0039-6028(02)01384-5
- Y.Q. Wang, R. Smirani, G.G. Ross, F. Schiettekatte, *Phys. Rev. B* **71**, 161310 (2005). doi:10.1103/PhysRevB.71.161310
- M. Brust, M. Walker, D. Bethell, D.J. Schiffrin, R. Whyman, *J. Chem. Soc. Chem. Commun.* **1994**, 801 (1994). doi:10.1039/c39940000801
- D.I. Gittins, F. Caruso, *Angew. Chem. Int. Ed.* **40**, 3001 (2001). doi:10.1002/1521-3773(20010817)40:16<3001::AID-ANIE3001>3.0.CO;2-5
- D. Shechtman, A. Feldman, J.L. Hutchison, *Mater. Lett.* **17**, 211 (1993). doi:10.1016/0167-577X(93)90001-E

14. D. Shechtman, A. Feldman, M.D. Vaudin, J.L. Hutchison, Appl. Phys. Lett. **62**, 487 (1993). doi:[10.1063/1.108915](https://doi.org/10.1063/1.108915)
15. J. Narayan, J. Mater. Res. **5**, 2414 (1990). doi:[10.1557/JMR.1990.2414](https://doi.org/10.1557/JMR.1990.2414)
16. W. Selke, P.M. Duxbury, Z. Phys. B Condens. Matter. **94**, 311 (1994). doi:[10.1007/BF01320684](https://doi.org/10.1007/BF01320684)
17. X. Yu, P.M. Duxbury, Phys. Rev. B **52**, 2102 (1995). doi:[10.1103/PhysRevB.52.2102](https://doi.org/10.1103/PhysRevB.52.2102)